

**Document Version**

Final published version

**Licence**

Dutch Copyright Act (Article 25fa)

**Citation (APA)**

Huang, Y., Zhang, H., Liu, X., Ma, B., & Huang, T. (2022). Iron-Activated Carbon Systems to Enhance Aboriginal Aerobic Denitrifying Bacterial Consortium for Improved Treatment of Micro-Polluted Reservoir Water: Performances, Mechanisms, and Implications. *ACS Environmental Science and Technology Water*, 56(6), 3407-3418. <https://doi.org/10.1021/acs.est.1c05254>

**Important note**

To cite this publication, please use the final published version (if applicable).  
Please check the document version above.

**Copyright**

In case the licence states "Dutch Copyright Act (Article 25fa)", this publication was made available Green Open Access via the TU Delft Institutional Repository pursuant to Dutch Copyright Act (Article 25fa, the Taverne amendment). This provision does not affect copyright ownership.  
Unless copyright is transferred by contract or statute, it remains with the copyright holder.

**Sharing and reuse**

Other than for strictly personal use, it is not permitted to download, forward or distribute the text or part of it, without the consent of the author(s) and/or copyright holder(s), unless the work is under an open content license such as Creative Commons.

**Takedown policy**

Please contact us and provide details if you believe this document breaches copyrights.  
We will remove access to the work immediately and investigate your claim.

# Iron-Activated Carbon Systems to Enhance Aboriginal Aerobic Denitrifying Bacterial Consortium for Improved Treatment of Micro-Polluted Reservoir Water: Performances, Mechanisms, and Implications

Yuwei Huang, Haihan Zhang,\* Xiang Liu, Ben Ma, and Tinglin Huang



Cite This: *Environ. Sci. Technol.* 2022, 56, 3407–3418



Read Online

ACCESS |



Metrics & More



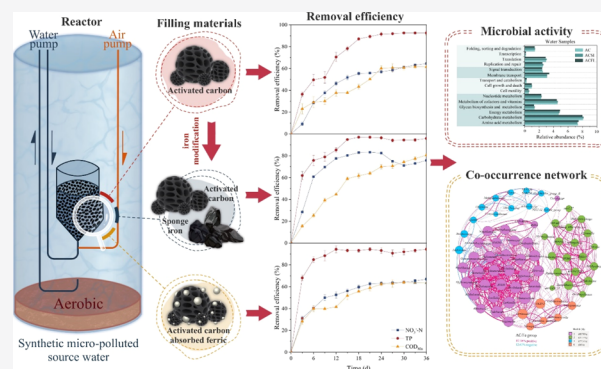
Article Recommendations



Supporting Information

**ABSTRACT:** Although many source waterbodies face nitrogen pollution problems, the lack of organic electron donors causes difficulties when aerobic denitrifying bacteria are used to treat micro-polluted water. Different forms of iron with granular activated carbon (AC) as carriers were used to stimulate aboriginal microorganisms for the purification of micro-polluted source water. Compared with the iron-absent AC system, targeted pollutants were significantly removed (75.76% for nitrate nitrogen, 95.90% for total phosphorus, and 80.59% for chemical oxygen demand) in the sponge-iron-modified AC system, which indicated that iron promoted the physical and chemical removal of pollutants. In addition, high-throughput sequencing showed that bacterial distribution and interaction were changed by iron dosage, which was beneficial for pollutant transformation and reduction. Microbial functions, such as pollutant removal and expression of functional enzymes that were responsible for the transformation of nitrate nitrogen to ammonia, were highly efficient in iron-applied systems. This study provides an innovative strategy to strengthen in situ remediation of micro-pollution in waterbodies.

**KEYWORDS:** aerobic denitrification, iron carbon, micro-pollution, microbial community, co-occurrence model



## 1. INTRODUCTION

With the development of industry and agriculture, surface waterbodies in rural and urban areas suffer from varying degrees of nitrogen pollution.<sup>1</sup> Micro-polluted reservoirs, in which the concentration of pollutants (i.e., nitrate, organic matter, etc.) is below 10 mg/L, often play a vital role in supplying water for industries, agriculture activities, and domestic drinking water.<sup>2,3</sup> The existence of nitrate in drinking water poses potential risks to human health and contributes to eutrophication, resulting in further deterioration of water quality.<sup>4–6</sup> Therefore, a novel treatment technology to deal with nitrogen pollution in lakes and reservoirs is an international research hotspot.

Microbial denitrification technology has been widely used in wastewater treatment because of its moderate price, high efficiency, and clean byproducts.<sup>5,6</sup> It involves two reactions: aerobic nitrification and anaerobic denitrification. Therefore, the presence of dissolved oxygen (DO) is an important inhibition in traditional denitrification. *Thiosphaera pantotropha* is the earliest identified aerobic denitrifier, and it possesses the ability of co-respiration or co-metabolism of oxygen and NO<sub>3</sub><sup>–</sup>,<sup>7</sup> indicating a significant latent capacity as a nitrogen removal method under oxic conditions.<sup>8</sup> Several aerobic

denitrifying bacteria have been isolated and identified with good nitrogen removal performance, including *Desulfovibrio* sp. CMX,<sup>9</sup> *Acinetobacter junii* YB,<sup>10</sup> and *Paracoccus denitrificans* ISTOD1.<sup>11</sup> However, these strains were isolated from or cultured in nutrient-rich conditions and were not intended to treat micro-polluted source water.

Aerobic denitrifiers are widespread in oligotrophic ecosystems.<sup>3,5,6,12,13</sup> The nitrate nitrogen (NO<sub>3</sub><sup>–</sup>-N) removal efficiency of 97.02% was reported in the Zhoucun reservoir during springtime through microbial aerobic denitrification, indicating that aerobic denitrification is successful in reducing nitrogen in micro-polluted water ecosystems.<sup>13</sup> Recently, many studies have focused on aerobic denitrifying bacteria in micro-polluted natural systems. For instance, the *Streptomyces* sp. Strain XD-11-6-2 isolated from the Jinpen reservoir efficiently removed nitrogen from reservoir water.<sup>3</sup> A mixed aerobic

Received: August 4, 2021

Revised: January 17, 2022

Accepted: February 16, 2022

Published: March 3, 2022



denitrifying consortium isolated from the Zhoucun reservoir achieved a  $\text{NO}_3^-$ -N removal efficiency of 75.32% in oligotrophic raw water.<sup>5</sup> However, a mixed-culture aerobic bacteria consortium isolated from a reservoir predominantly containing *Sphingomonas sanxanigenes* and *Rhodobacter blasticus* achieved the highest nitrate removal efficiencies of 94.97% in the denitrification medium but only 35.6% in source water because of insufficient organic matter content.<sup>6</sup>

To solve the issue of the shortage of organic electron donors in micro-polluted water, the addition of inorganic substances (i.e., hydrogen, sulfur, and sulfur compounds and zero-valence or low-valence metals) as electron donors can strengthen denitrification.<sup>1</sup> Zero-valent iron (ZVI) is an abundant, inexpensive, and relatively innocuous material that improves microbial reactivity.<sup>14–16</sup> In addition to providing electrons directly to the denitrifiers, iron also generates hydrogen ( $\text{H}_2$ ) and  $\text{Fe}^{2+}$  to strengthen denitrification.<sup>17</sup> As a necessary trace element for bacterial growth, iron can also promote microbial physiological activity.<sup>18</sup> In addition, the chemical reaction of iron can also reduce nitrogen and phosphorus content directly.<sup>16,19</sup>

However, iron corrosion is relatively slow and unsustainable, especially under neutral and alkaline conditions.<sup>9,14</sup> Hence, the Fe/AC micro-electrolysis process is an effective method. In the Fe/AC micro-electrolysis system, substantial quantities of microscopic galvanic elements are produced by the contact between ZVI and AC.<sup>20</sup> The Fe/AC micro-electrolysis-modified iron-based denitrifying system shows a fast and high nitrogen removal ability.<sup>21</sup> Consequently, the application of iron and AC to enhance denitrification is potentially feasible for the in situ treatment of oligotrophic water. However, this technology has scarcely been implemented for the treatment of micro-polluted natural water, causing difficulties for practical engineering applications.

The general aim of this work is to explore the mechanisms of iron-AC systems to enhance aboriginal aerobic denitrifying bacterial consortium for improved treatment of micro-polluted reservoir water based on microbial ecology characteristics. To this end, the specific objectives of this study were to (1) evaluate the removal performances of nitrate and other pollutants from micro-polluted water, (2) analyze the pathways of iron compounds, (3) analyze the shifts in microbial community structure and metabolic functional patterns using 16S rRNA gene sequencing, and (4) evaluate the interspecific interactions of mixed-culture microbial communities by network analysis. Overall, this study aims to provide an innovative strategy to enhance aboriginal aerobic denitrification for the in situ treatment of micro-polluted water and a theoretical basis for engineering applications.

## 2. MATERIALS AND METHODS

**2.1. Raw Materials and Microorganisms.** Sponge iron (s-ZVI) (Henan Boyuan Water Purification Materials Co., Ltd, Henan, China), with a diameter of 3–5 mm, unit weight of 2.2 g/cm<sup>3</sup>, specific surface area of 85 m<sup>2</sup>/g, and content of active iron greater than 88%, was prepared by washing with diluted  $\text{H}_2\text{SO}_4$  solution and deionized water to scour off the oxide coating on the surface. Granular AC was obtained from Jiangsu Zhikang Carbon Technology Co., Ltd, Jiangsu, China, with a granularity of 8–16 mesh (1.00–2.36 mm), bulk density of 0.75 g/cm<sup>3</sup>, and specific surface area of 285 m<sup>2</sup>/g, and was rinsed with distilled water 3 times before use. The ferric-modified AC was prepared by immersing a part of washed AC

in 100 g/L  $\text{FeCl}_3$  for 24 h and washing repeatedly with distilled water. All carbon materials were finally dried to a regular weight at 80 °C.

The sediment and raw water were collected from the Jinpen reservoir (33°51' N to 34°08' N; 109°17' E to 109°36' E), located in the city of Xi'an, Shaanxi Province, Northwest China, during autumn time in 2020. Due to the low concentration of N and P in raw water, synthetic micro-polluted source water was prepared in this study by adding  $\text{KNO}_3$  and  $\text{KH}_2\text{PO}_4$ . Based on the previous reports of drinking water reservoir in China during summer, the concentrations of 2.5 mg/L of  $\text{NO}_3^-$ -N and 0.16 mg/L of TP were used in this study.<sup>2,13,22</sup> The chemical characteristics of raw water are described in Table S1.

Prior to the experiment, 20 L of sediment and 40 L of synthetic micro-polluted source water were mixed and cultivated in a continuous mixing aerobic reactor (DO concentration at 7–9 mg/L) to enrich the mixed culture of aboriginal denitrifying bacteria. The reactor was constantly fed with  $\text{CH}_3\text{COONa}$ ,  $\text{KNO}_3$ , and  $\text{KH}_2\text{PO}_4$  every 2 days to maintain the nutrient concentration [nitrate nitrogen concentration ranged from 3 to 4 mg/L, chemical oxygen demand by potassium permanganate ( $\text{COD}_{\text{Mn}}$ ) = 6–8 mg/L, and total phosphorus (TP) = 0.2–0.3 mg/L]. After 1 month of cultivation, with the stable total cell concentration at  $10^9$  CFU/mL in water (filtered by 5  $\mu\text{m}$  polycarbonate membrane filter), the mixed aboriginal bacterial consortium was collected and rinsed to prepare bacterial suspension for further experiment.

**2.2. Experimental System Configuration and Operation.** Three aerobic denitrifying reaction systems—AC system, AC with sponge iron system (ACSI), and AC absorbed ferric iron system (SCFI)—were established in the laboratory at Xi'an University of Architecture and Technology, China. Each reaction unit was uniformly assembled by a cylindrical PVC tube with an inner diameter of 200 mm and a height of 1000 mm. The layout of the reaction system is shown in Figure S1. The fillers of AC, ACSI, and SCFI reactors contained 175 mL AC, 175 mL AC with 80 g s-ZVI, and 175 mL ferric-modified AC, respectively.

The water and air pipe outlets were connected to the reactor to ensure adequate mixing of water and adjust the DO concentration. The inlet of the water pipe was fixed above the sediment surface to prevent disturbance to sediment. After establishing all reaction units, 1% (v/v) of the bacterial suspension was seeded into the units within 24 h after collection. All systems with a working volume of 30 L synthetic micro-polluted source water and 1.6 L sediment were operated for 36 days under continuous aeration and water circulation at the room temperature of  $23 \pm 2.5$  °C. DO concentration of the reactors was controlled between 7 and 9 mg/L during the operation.

**2.3. Measurements of Chemical Water Quality Parameters.** The concentrations of  $\text{NO}_3^-$ -N, nitrite-nitrogen ( $\text{NO}_2^-$ -N), ammonium-nitrogen ( $\text{NH}_4^+$ -N), TN, and TP were detected using a spectrophotometer (UV-2600, UNICO, USA). Except TN, TP, and total iron concentrations, all samples were filtered with 0.45  $\mu\text{m}$  polycarbonate membrane filters (Jinteng, Tianjin, China). The above parameters and  $\text{COD}_{\text{Mn}}$  were measured in accordance with the standard method and protocol of the State Environment Protection Administration of China (SEPA, 2002). AA6800 atomic absorption spectroscopy (Shimadzu, Japan) was used to

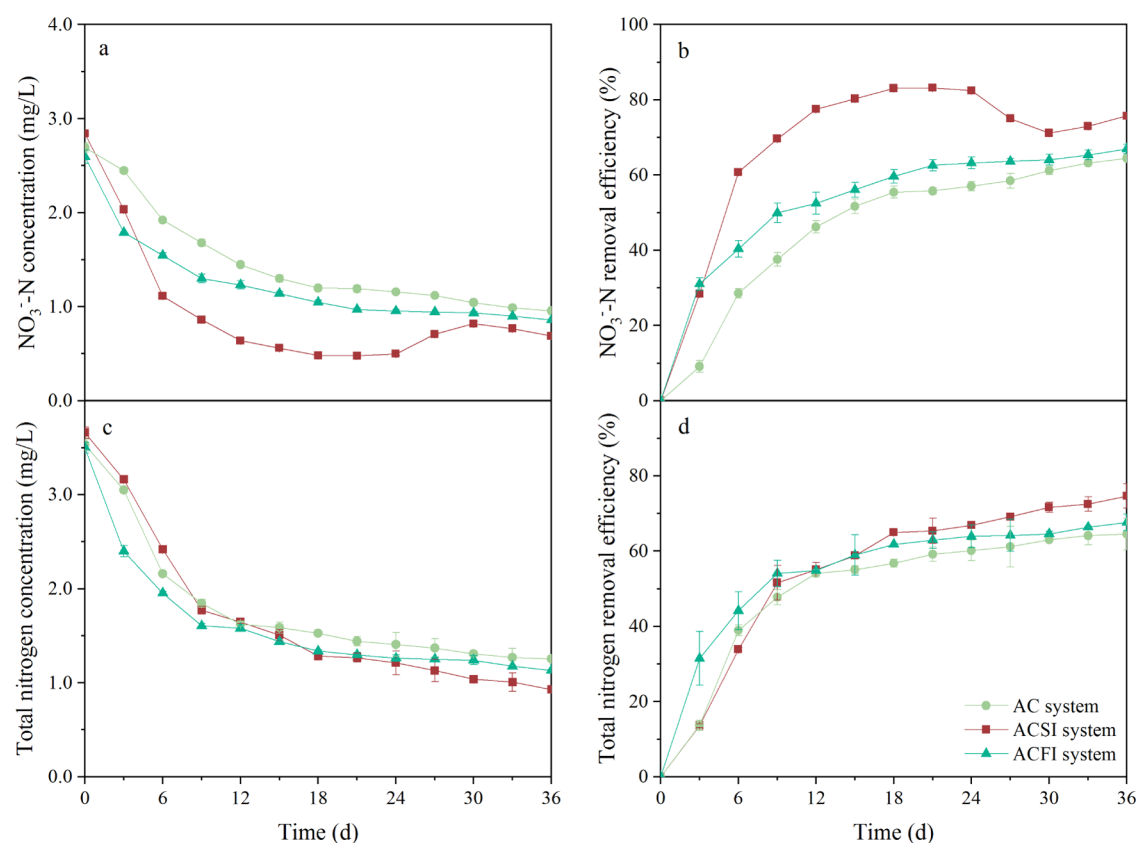


**Figure 1.** Nitrogen removal performance of AC, ACSI, and ACFI systems during the experimental operation. Variations in NO<sub>3</sub><sup>-</sup>-N concentration and removal efficiency (a,b); variations in TN concentration and removal efficiency (c,d).

measure the total iron concentrations. DO concentration and water temperature were detected using a portable DO probe and thermometer (DO-957, Leici, China). pH value was measured by a pH meter (STARTER 3100/B, OHAUS, USA). The above water quality parameters were measured every 3 days to evaluate the pollutant removal performance of the system. Turbidity was detected by a portable turbid meter (WGZ-1A, Xinrui Instrument, China) at the start and the end of the experiment. All measurements were conducted in triplicate ( $n = 3$ ).

**2.4. Genomic DNA Extraction.** One liter of water was filtered through 0.22  $\mu\text{m}$  sterilized polycarbonate membrane filters (Jinteng, Tianjin, China), and 10 mL sediment of each system was collected for DNA extraction to characterize the microbial community. The genomic DNA was then extracted using a Water DNA kit (OMEGA, Irving, TX, USA) by following the manufacturer's instruction and purified using the AxyPrep DNA Gel Extraction Kit (Axygen Biosciences, Union City, CA, USA). All the samples were stored at  $-80\text{ }^{\circ}\text{C}$  until they were used for polymerase chain reaction (PCR) amplification analysis.<sup>13</sup>

**2.5. High-Throughput DNA Sequencing and Analysis.** An Illumina MiSeq platform (Majorbio Bio-pharm Technology Co., Ltd., Shanghai, China) was used for high-throughput DNA sequencing of 16S rRNA gene in the DNA extracted from water and sediment samples. 16S rRNA genes were amplified by a PCR instrument (9700, GeneAmp ABI, USA) using the primers 338F (5'-ACTCCTACGGGAGGCAG-CAG-3') and 806R (5'-GGACTACHVGGGTWTCTAAT-3').<sup>13</sup>

The 16S rRNA gene sequences were analyzed using the CASAVA base recognition analysis and then stored as a FASTQ file. The sequences with a similarity of 97% were classified to the same operational taxonomic units (OTUs) that were used to compute the diversity index using Mothur v.1.30.1 (<http://www.mothur.org/>).<sup>23</sup> Before further analysis, all samples were normalized to the same sequencing depth by randomly removing the redundant reads to guarantee fair comparison.<sup>13</sup> The amplified sequences were compared with the KEGG database (<http://www.genome.jp/kegg/>) to employ the Phylogenetic Investigation of Communities by Reconstruction of Unobserved States (PICRUSt) and uploaded to the NCBI database (<http://www.ncbi.nlm.nih.gov/>).

**2.6. Statistical Analysis.** The 16S rRNA sequences analysis was performed using the Majorbio Cloud Platform (<http://www.majorbio.com>). The statistical analysis was performed using SPSS Statistics 22.0. The OriginPro 2018 software was used for drawing figures. The R 4.0.5 and Gephi 0.9.3 software were used for network analysis and visualization. Based on the *t*-test, the differences were regarded as significant at  $P < 0.05$ , and error bars represent  $\pm 1$  standard deviation.

### 3. RESULTS AND DISCUSSION

**3.1. Aerobic Denitrification Performance and Role of Iron.** In recent years, many strains of aerobic denitrifiers have been found to have a high nitrate removal capacity in media with high nitrate concentrations.<sup>9–11</sup> However, they have an unsatisfactory capacity to treat raw water because of their weak resistance to environmental loads and insufficient nutrients.<sup>3</sup> Previous studies found that a mixed-aerobic denitrifying

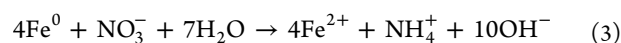
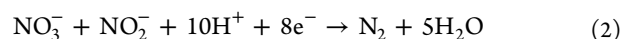
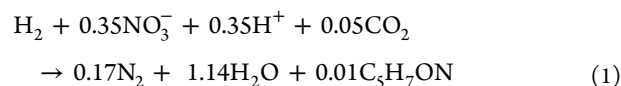
consortium presented significantly higher  $\text{NO}_3^-$ -N removal efficiency and better response to environmental changes than that of a single strain, which might be attributed to an efficient and complete nitrogen cycle caused by interspecies interactions.<sup>5,22</sup> Thus, in contrast to previous investigations, this study added iron as inorganic electron donors directly into the raw water to enhance the nitrogen removal ability of the aboriginal mixed bacteria consortium without using an artificial denitrification medium. The variation in nitrogen concentration indicates the potential of the iron-enhanced aboriginal aerobic denitrification process for in situ remediation of micro-polluted water.

The variations in the concentrations of  $\text{NO}_3^-$ -N and total nitrogen (TN) and nitrogen removal efficiencies were analyzed to determine the denitrification capacities of the three systems (Figure 1). The concentrations of TN and nitrate decreased drastically for the first 6 successive days and continued to decrease moderately from the 6th to the 36th day. The AC system presented the lowest  $\text{NO}_3^-$ -N removal efficiency of 64.49% compared to the other systems that were modified with inorganic electron donors. Although the concentration of  $\text{NO}_3^-$ -N in the ACSI system showed a 0.32 mg/L increase from the 24th to 30th day, which was different from other systems, the highest reduction rate of nitrate (75.76%) among the three systems was observed at the end of the operation. TN concentration variations were similar in all systems, showing a significant reduction. The ACSI system showed the best total nitrogen removal efficiency (74.65%), followed by the ACFI system (67.63%) and the AC system (64.54%). Compared with the AC system, the  $\text{NO}_3^-$ -N removal efficiencies were improved by 17.48 and 3.85% in the ACSI and ACFI systems, respectively. The nitrogen reduction ability was significantly promoted by iron dosage ( $P < 0.001$  in the ACSI system and  $P < 0.05$  in the ACFI system). These results suggest that although iron can have mild toxicity to microorganisms, it promotes nitrogen removal efficiency in aerobic systems, which is consistent with previous studies.<sup>24,25</sup> Supplementation of iron was reported to promote denitrification in many previous studies. According to previous studies,<sup>16,26</sup> adding ferrous ions improved TN removal efficiency by 3.71% in constructed wetlands (CW) and 4.31% in biofilter, respectively. Sponge iron reported to increase nitrate removal efficiency by 16–76% in CW (depending on the influent nitrate concentration).<sup>24</sup>

The variations in  $\text{NO}_2^-$ -N and  $\text{NH}_4^+$ -N concentrations are shown in Figure S2. All the three systems exhibited accumulations of  $\text{NO}_2^-$ -N and  $\text{NH}_4^+$ -N in the early stages of biotic and abiotic denitrification and were consistent with the observations reported in other studies.<sup>9,15</sup> The concentrations of  $\text{NO}_2^-$ -N in the AC and ACSI systems peaked at 0.045 and 0.063 mg/L, respectively, after 3 days of operations. In the ACFI system, the increase in  $\text{NO}_2^-$ -N concentration continued for 6 days and reached 0.136 mg/L. The concentration of  $\text{NH}_4^+$ -N in all systems peaked on the third day. The ACSI system produced more ammonia with the highest concentration of 0.83 mg/L. Although the ammonia concentration dropped to about 0.14 mg/L in the other two systems on the 6th day, it did not decline until the 12th day and then remained stable at 0.67 mg/L in the ACSI system.

The pH variations during the operations are provided in Figure S3. During the first 6 days, the alkalinity in the three systems increased owing to the production of hydroxide ions during denitrification (eqs 1–3).<sup>14,23</sup> The pH value was about 8.06 in the iron-containing systems after the 6th day, while the

AC system showed a more alkaline environment. It was reported that ZVI and  $\text{Fe}^{2+}$  can reduce the pH of alkaline systems due to the reaction between  $\text{OH}^-$  and iron ions,<sup>9</sup> which also theoretically explains the low total iron concentration ( $<0.030$  mg/L and mean value of 0.014 mg/L) during the experiment.



According to the variation in nitrogen and pH value, iron promoted the nitrogen removal ability probably because of the enhancement in both abiotic and biotic denitrification.<sup>24,25</sup> However, most of the present studies on nitrate reduction with iron are under anaerobic conditions. Although oxygen influenced the oxidative dissolution of ZVI to produce ferrous ions, the produced ferrous ions reduced the DO concentration to produce ferric ions, keeping the overall electron efficiency uninfluenced.<sup>15</sup> Thus, abiotic denitrification efficiency using iron is relatively immune to DO concentrations, and the conclusions obtained under anaerobic conditions can also be used to prove the results in an aerobic environment.

According to a previous study,<sup>27</sup> substantial  $\text{NO}_2^-$ -N was produced during the reaction of ferric and ferrous hydroxides with  $\text{NO}_3^-$ -N and accumulated by the hysteresis of the nitrite reduction into gaseous nitrogen or ammonium, which is similar to the variation in nitrite concentration in the ACFI system.<sup>4</sup> This was attributed to the incomplete nitrate reduction that occurred when ferric and ferrous compounds reacted with nitrate, which was inclined to generate nitrite.<sup>15</sup>

According to the variation in different forms of nitrogen, the denitrification process of the ACSI system can be divided into three stages: (1) at 0–3 days, it was dominated by the chemical reduction of nitrate by ZVI. The nitrate concentration decreased by 0.81 mg/L, and the ammonia concentration increased by 0.64 mg/L at this stage. ZVI could hardly react with nitrate but could promote the chemical reaction of nitrite to ammonium under a neutral pH condition.<sup>9</sup> However, Fe/AC showed a wider pH range for the chemical reaction of ZVI with nitrate that TN removal efficiency kept higher than 35% with pH lower than 9.0 with main production of ammonia.<sup>25</sup> Also, it was attributed to the limited capacity of ZVI in the selective transformation of nitrate to nitrogen gas. The s-ZVI particles contained a certain amount of elemental carbon after sintering at a high temperature, whose composition was distinctly different from that of ZVI, thereby creating a ZVI/C micro-electrolysis system to form massive galvanic elements.<sup>24</sup> Furthermore, sponge iron was porous; compared with the commonly used ZVI (i.e., iron beads, scraps, shavings, etc.), the specific surface area of sponge iron was much larger, thus contributing to more pronounced chemical reaction properties and significant ammonia generation. Moreover, because the chemical reaction is faster than the biological reaction, leading to the obvious accumulation of ammonia nitrogen in this stage. (2) During 3–24 days nitrate was mainly reduced by the biological denitrification promoted by ZVI; ammonia, nitrite, and nitrate nitrogen concentrations showed a slow decreasing trend. In addition to the improvement in chemical denitrification, ZVI

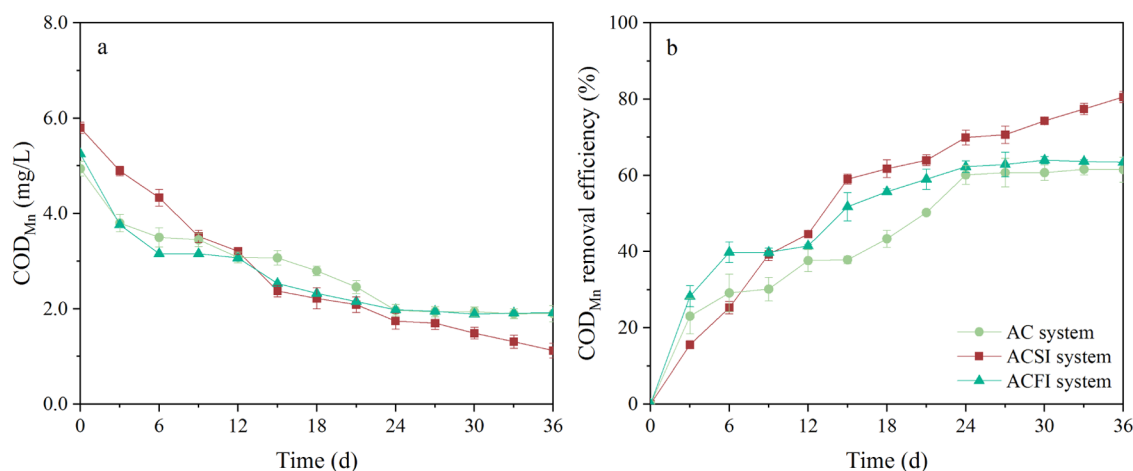


**Figure 2.** Organic matter removal performance of AC, ACSI, and ACFI systems during the experimental operation. Variations in COD<sub>Mn</sub> concentration (a) and removal efficiency (b).

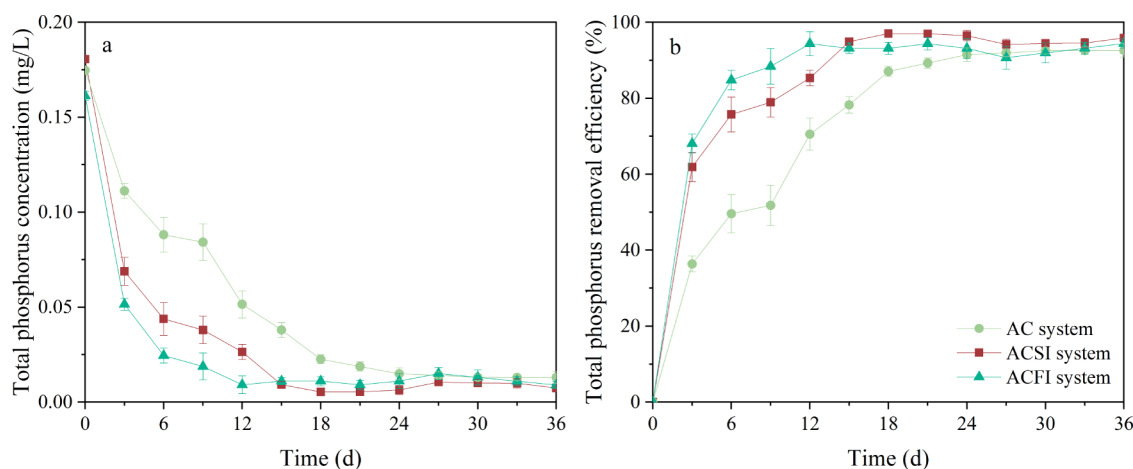


**Figure 3.** Phosphorus removal performance of AC, ACSI, and ACFI systems during the experimental operation. Variations in TP concentration (a) and removal efficiency (b).

also promotes the biological denitrification by rendering additional electron sources.<sup>9</sup> Ferrous ions and hydrogen produced by immersed iron can also be used by biotic denitrifiers to remove NO<sub>3</sub><sup>-</sup>-N.<sup>24</sup> Also, iron has been verified to influence the bacteria community structure, which was associated with the simultaneous nitrification and denitrification appearance.<sup>28</sup> Furthermore, iron was also reported to facilitate the attachment of microorganisms by roughening the ZVI surface,<sup>29</sup> stimulate the production of extracellular polymeric substances to promote microbial aggregation,<sup>30</sup> improve the hydrophilicity of ZVI, and provide positively charged ions (i.e., Fe<sup>3+</sup> and Fe<sup>2+</sup>) on AC to draw negatively charged microbes.<sup>18</sup> (3) On 24–36 days, there was the acceleration of heterotrophic denitrification function by aerobic denitrifying bacteria. Nitrification transformed NH<sub>4</sub><sup>+</sup>-N into nitrate, and then it was converted to nitrogen gas by denitrifying bacteria, causing a drastic decrease in the concentration of ammonia and an increase in nitrate concentration at the later stage of operations.

Overall, NO<sub>3</sub><sup>-</sup>-N is mainly reduced biotically in iron-modified systems in accordance with previous findings.<sup>15</sup> This also demonstrated the reason for the much lower abiotic denitrification efficiency of Fe/AC micro-electrolysis; even using nano-ZVI with high chemical reactivity achieved a

maximum removal efficiency of only 38.9% (initial pH of 7.0 and nitrate concentration of 20 mg/L).<sup>25</sup> Therefore, the iron-modified system promoted the denitrification in both abiotic and biotic ways, and the ACSI system exhibited the best denitrification performance.

**3.2. Removal of Organic Matter.** Organic matter can provide aerobic denitrifying bacteria with essential energy and electrons for reproduction and metabolism.<sup>22</sup> Figure 2 shows the variations in COD<sub>Mn</sub>, and its removal efficiencies were 80.59% in the ACSI system and 61.53% in the AC system on the 36th day. The results of the *t*-test show that the removal efficiencies in both ACSI and ACFI systems were significantly higher than those in the AC system, with *P* values less than 0.001 and 0.05, respectively, exhibiting excellent removal capacities for organic matter. The majority of aerobic denitrifying bacteria showed high carbon removal efficiency. In theory, a reduction of 3.6 mg/L (COD<sub>Mn</sub>) of organic carbon in the three systems can cause a decrease in NO<sub>3</sub><sup>-</sup>-N by 1.4 mg/L through the traditional heterotrophic denitrification process, which is lower by 0.4 mg/L compared to the removal achieved by the experiment. Therefore, the denitrification process that occurs in this study is likely to involve processes other than the heterotrophic process such as autotrophic denitrification and dissimilatory nitrate reduction to ammo-

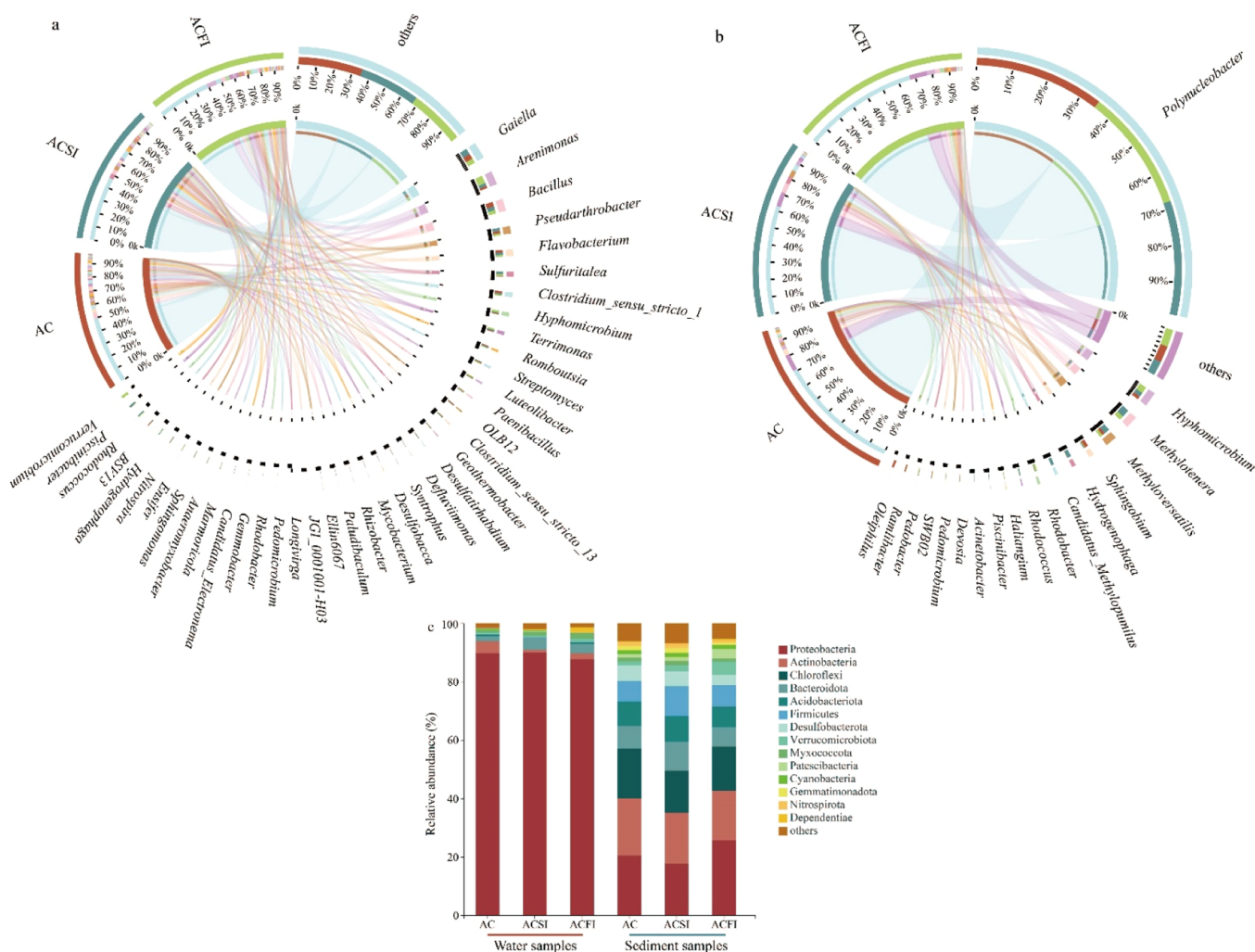


**Figure 4.** Microbial community composition in AC, ACSI, and ACFI systems at the end of operation based on Illumina MiSeq sequencing of 16S rRNA. Microbial composition at the genus level of sediment (a) and water samples (b). Microbial composition at the phylum level of water and sediment samples (c). The microbes with population less than 0.01 were merged with others.

nium process.<sup>31</sup> Moreover, based on the Pearson's correlation indices of all systems, it is evident that nitrate removal was significantly positively related to  $\text{COD}_{\text{Mn}}$  removal. The correlation coefficient value in the AC system was consistent with the denitrification process of other aerobic denitrifiers such as *Streptomyces* sp. XD-11-6-2,<sup>3</sup> and a consortium of mixed-culture aerobic denitrifying bacteria.<sup>6,22</sup> In addition, the  $r$  values of the ACSI was 0.835, lower than 0.937 of the AC system ( $P < 0.01$  and  $n = 13$ ), indicating that organic carbon provided the primary electron donor to the denitrifying bacteria to facilitate the removal of nitrogen, especially without the inorganic electron donor supplement.

**3.3. Removal of Phosphorus.** Phosphorus pollution contributes to eutrophication as it facilitates microbial growth. Therefore, this study also explored the dephosphorization abilities of the systems. Waterbodies contain phosphorus in dissolved and particulate forms, and these forms are mutually interchangeable based on their conditions and functions of aquatic organisms present in them.<sup>32</sup> The concentration of TP continuously decreased (Figure 3), and it eventually achieved a significant removal rate of >90% in all systems. The removal efficiencies were significantly faster in the iron-supplied systems at 94.92 and 93.16% on the 15th day in the ACSI and ACFI systems, respectively, than in the AC system at

78.26%. In general, the presence of iron accelerates the removal rate of phosphorus. A previous study also noted that the combination of iron and carbon improved the removal performances of both nitrogen and phosphorus in CW.<sup>23</sup>

In aqueous solutions consisting of iron (ACSI and ACFI systems), the rapid phosphorus removal rate can be attributed to abiotic pathways, including physical adsorption and chemical precipitation.<sup>19</sup> On the one hand, ZVI generated positively charged iron oxide ( $\text{Fe}_2\text{O}_3$  and  $\text{Fe}_3\text{O}_4$ ) surfaces, providing sites for the absorption of phosphates or anionic compounds.<sup>33</sup> Adsorption was probably the main pathway to remove TP in the early stage of operation in the ACSI system because this reaction dominates in ZVI-supplied phosphorus removal when iron with large specific surface areas was used in the experiment.<sup>19</sup> On the other hand, for the corrosion products of iron, ferrous and ferric ions were generated with a longer duration of operation. After the formation of  $\text{Fe}(\text{OH})_2$  and  $\text{Fe}(\text{OH})_3$ , they reacted with P to form chemical precipitates.<sup>34</sup> Therefore, precipitation might be the major chemical mechanism of TP removal in the ACFI system and in the later stages of the ACSI system. For the AC system, the turbidity dropped from 9.9 NTU at the beginning to 3.8 NTU at the end of the operation, indicating that dephosphorization was probably attributed to physical sedimentation of

**Table 1. Bacterial Richness and Diversity Estimators of Water and Sediment Samples in AC, ACSI, and ACFI Systems at the End of Operation**

sample ID		0.97 level					
		OTUs	ACE	Chao	Shannon	Simpson	coverage
sediment	AC	2446	2858	2864	6.41	0.0058	0.983
	ACSI	2409	2661	2669	6.55	0.0041	0.987
	ACFI	2400	2675	2658	6.35	0.0055	0.985
water	AC	408	445	390	2.10	0.3786	0.997
	ACSI	480	513	493	2.95	0.1628	0.997
	ACFI	503	577	535	2.74	0.2490	0.995

particulates with phosphorus and adsorption of dissolved phosphorus by suspended particles. However, the speed of this process was much slower than that of the chemical reaction; thus, the TP concentration showed a gentler downward trend compared with those of the other systems.

However, in the ACFI system, owing to the relatively low TP concentration, the phosphorus removal efficiencies by iron modification at the end of the experiment did not improve significantly ( $P > 0.05$ ).

**3.4. Variation in Bacterial Community Composition and Structure.** Figure 4a,b shows the compositions of bacterial communities at the genus level present in the sediment and water samples, respectively, in the AC, ACSI, and ACFI systems. The microbial compositions of the sediment samples in the three systems were similar with no specific dominant strain, and the highest proportion of abundance was by *Gaiella* at 5%. However, the distributions of the microbial communities in the water samples were significantly different from that in the sediment with *Polynucleobacter*, accounting for approximately 90% of the total. *Polynucleobacter*, a genus of aerobic heterotrophic bacteria with small cell sizes ( $<0.1 \mu\text{m}^3$ ), were ubiquitous in freshwater ecosystems covering almost the entire range of trophic levels.<sup>35</sup> However this bacterium does not participate in the nitrogen cycle.<sup>36</sup> The ultra-micro size of *Polynucleobacter* is probably the cause for its high abundance with respect to the total quantity of microbes. *Hyphomicrobium*, *Methylotenera*, and *Methyloversatilis* were known as major players in aerobic denitrification systems that were supplied with methanol as a carbon source.<sup>37–39</sup> *Hyphomicrobium* was also reported as the manganese oxidizing bacteria that was found in a biofilter developed for Fe, Mn, and As(III) removal<sup>40</sup> and identified as the main microbe responsible for Fe and Mn-oxidation in a slow sand filter.<sup>41</sup> Therefore it showed a relatively high abundance in iron-modified systems. *Methylotenera* almost only presented in iron-modified systems; this result was consistent with the previous study that ZVI increased the abundance of *Methylotenera* in a biological nitrate removal system.<sup>17</sup> The relative abundance of *Methyloversatilis* was significantly improved in the ACSI system, which has been proved to “switch” from heterotrophy to autotrophy by using inorganic electron donors (hydrogen or iron) when organic matter is insufficient.<sup>37,38</sup> In addition, *Hydrogenophaga* are facultative aerobic autotrophic denitrifying bacteria using [H] or  $\text{H}_2$  as electron donors.<sup>9,37</sup> *Hydrogenophaga* almost only presented in the ACSI system but were absent in others, which is consistent with the previous study.<sup>42</sup> In the ZVI-modified system, the produced ferrous ions and hydrogen were released by immersed iron and used by *Hydrogenophaga*, which could explain this phenomenon.<sup>24</sup> Overall, the highest presence of *Methylotenera* and *Hydrogenophaga* in the ACSI system

indicated the occurrence of autotrophic denitrification. However, the heterotrophic denitrifiers were still dominated in all systems, and their abundance was increased in iron-modified systems, which demonstrated that iron promoted both heterotrophic and autotrophic denitrification, with heterotrophy being dominant.

Cluster analysis at the phylum level in the sediment and water samples of the three systems (Figure 4c) showed that the compositions of microbes in the sediment were more well distributed than those in water and predominantly contained *Proteobacteria* (17.59–25.64%), *Actinobacteria* (17.13–19.54%), *Chloroflexi* (14.41–17.08%), *Bacteroidota* (6.67–9.84%), *Acidobacteria* (7.06–8.76%), and *Firmicutes* (6.97–10.21%). Overall, with the dosage of iron, the abundance of most of the microbes in the sediments of the three systems did not change after 1 month of operation, indicating that iron had a minor effect on microbial species in sediments. Moreover, *Cyanobacteria* were almost negligible in all water samples (0.10–0.47%), and sediment samples contained marginally higher quantities (1.24–1.44%) possibly due to their settlement after death, which was caused by the insufficient illumination in the opaque reactors.

The prevailing populations at the phylum-level abundances of bacteria in the water samples were significantly different from those of the sediment, including *Proteobacteria* (87.68–90.00%), *Actinobacteria* (0.92–4.09%), and *Bacteroidota* (1.64%–4.07%). *Proteobacteria* contain an abundance of microbes responsible for the removal of  $\text{COD}_{\text{Mn}}$ , N, and P (i.e., ammonia-oxidizing bacteria, nitrite-oxidizing bacteria, denitrifiers, and polyphosphate-accumulating organisms).<sup>43</sup> *Bacteroidota* and *Chloroflexi* have also been shown to contain dominant nitrogen- and iron-cycling bacteria.<sup>44</sup> Figure 4c shows that the dosage of s-ZVI and ferric ion restrained the propagation of *Actinobacteria* but promoted the growth of *Bacteroidota* in the water. A similar variation was also reported by a previous study,<sup>23</sup> indicating that iron is advantageous for the growth of *Bacteroidota*. In addition, the proportion of the abundance of *Dependentiae* increased from 0.29% in the AC system to 0.31% in the ACSI system and 1.58% in the ACFI system. This phylum was classified as facultative anaerobic, and its abundance was positively correlated with iron concentration.<sup>45</sup> Hence, iron stimulated aerobic denitrifying bacteria and consequently promote the N-removal capacity of the ecosystem.

The alpha-diversity estimators of the water and sediment samples from the three systems are shown in Table 1. A coverage index of >98% indicates the reliability of the high-throughput sequencing data. The Chao and ACE indices reflect the quantity of species, with higher values indicating higher abundance. The Shannon and Simpson indices reflect microbial diversity, whose numerical sizes show positive and

negative correlations with microbial diversity, respectively.<sup>23</sup> The richness and diversity estimators of the water and sediment samples that were influenced by iron addition showed different results. The alpha-diversity estimators of the sediment samples show that iron suppressed microbial richness, while the influence of iron on bacterial diversity in the sediment is unclear. Based on the indices of the water samples, it was evident that iron dosage (ZVI,  $\text{Fe}^{2+}$ , and  $\text{Fe}^{3+}$ ) significantly increased the richness and diversity of microbial flora, which is in agreement with the conclusion that iron supplementation into CWs promoted the Chao1, Simpson, and Shannon indices.<sup>26</sup> However, several studies have concluded that ZVI causes a decrease in microbial richness and diversity in wastewater treatment<sup>18</sup> and CWs,<sup>23,24</sup> which is probably due to the physicochemical environment created by iron, carbon source, or some other factors that are more conducive to some microorganisms compared to others. Therefore, the variety of richness and diversity estimators were the outcomes of the differences in many influencing factors, which were not limited to the impact of iron.

Network analysis is an advanced method for analyzing correlations between functional bacteria. Co-occurrence analysis at the gene level was evaluated by network inference based on Spearman's coefficient  $R > 0.6$  and  $P < 0.05$ . The three systems were divided into AC group (containing the AC system) and Fe/AC group (containing the ACSI and ACFI systems) according to whether iron was added. Seventy genera with the highest relative abundance in the water samples were utilized in the analysis and are shown in Figure 5. The topological parameters of the network are provided in Table 2.

As shown in Figure 5, 690 edges were calculated (75.94% positive and 24.06% negative) for bacteria in the AC group and 713 edges (87.83% positive and 12.62% negative) for bacteria in the Fe/AC group. Positive associations revealed cross-feeding, co-aggregation, co-colonization, and niche overlap between microbes, whereas negative correlations indicated differences in growth constraints among bacteria or antagonism.<sup>46</sup> More negative links in the AC group than in the Fe/AC group suggested that more competitive associations might be found in an iron-absent environment.<sup>47</sup> The degree of nodes typically characterizes the number of direct association interactions for a specific node. The path length (or geodesic distance) reveals the shortest path between two individual nodes.<sup>48</sup> As the path length shortens, the exchange rate of information, energy, and substances between microbes increase. A lower average path length and network diameter were observed in the Fe/AC group, suggesting that iron dosage likely led to a more intensive network interaction and faster inter-biological functions. In addition, the network of the Fe/AC group was more complex than that of the other group, as it exhibited a higher graph density and higher average node degree.<sup>46</sup> The increasing complexity of the community would be beneficial for improving the stability of the microbial community combined with mixed interaction types. Moreover, the ratio between network density ( $D$ ) and clustering coefficient ( $CC$ ) can also represent the stability of the networks, and the smaller the number, the higher the stability.<sup>49</sup> The ratio of the Fe/AC group ( $D/CC = 0.123$ ) was lower than that of the AC group ( $D/CC = 0.332$ ), which supports the conclusion that the stability of iron-modified systems was higher than that of iron-absent systems. The higher stability indicated that the microbes in iron-added ecosystems would be more resistant to variations in the

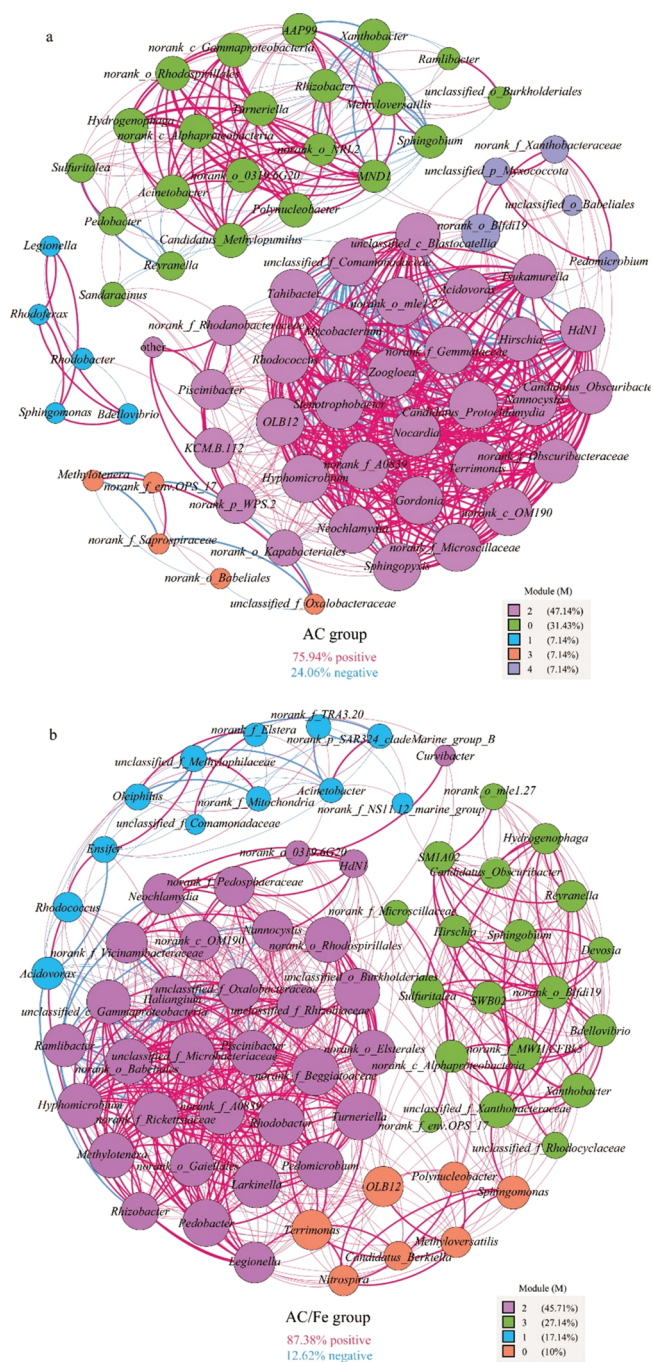


**Figure 5.** Co-occurrence network visualizing the correlations among species in the AC system (a) and Fe/AC systems (ACSI and ACFI systems) (b). Symbol sizes are proportional to the degree of nodes, and node colors represent the modules of different microbial groups. Larger size indicates a higher degree and more edge connections. Red edges represent the positive associations, and blue edges represent the negative associations.

environment. In general, iron might be an important factor in maintaining biodiversity and stability of the ecological community; thus, iron addition can promote the removal of specific pollutants.<sup>50</sup>

Furthermore, the microbes that were more related to others were placed in the middle of the network; on the contrary, those that were less related were placed on the edge.<sup>47</sup> However, the genera with relatively high abundances among microbial communities were observed with relatively low node

**Table 2. Network Parameters of the Correlations among Species in AC System and Fe/AC Systems (ACSI and ACFI Systems) ( $R > 0.6$ ,  $p < 0.05$ )**

network parameters	systems	
	AC system	Fe/AC system
nodes	70	70
edges	690	713
average degree	19.714	20.371
average weighted degree	31.251	25.787
network diameter	9	6
graph density	0.286	0.295
modularity	0.386	0.387
connected components	2	1
average clustering coefficient	0.861	0.775
average path length	2.859	2.299

proportions and were located at the margin of the network. For instance, the top populations in the AC group, including *Polynucleobacter* and *Sphingobium*, were not in the center and at a degree of only 18 and 17, respectively. Therefore, some predominant species did not play the same important role in microbial co-occurrence as in the composition.

**3.5. Variation in Microbial Activities.** As shown in Figure 6, the PICRUSt software predicted microbial potential functions at the genetic level, further exhibiting the variation in bacteria. Overall, 11 of 15 selected level 2 KEGG pathways were stimulated in iron-modified systems in water samples. Metabolism pathways are necessary for the survival of microorganisms. Among them, the top three potential functions, including metabolisms of carbohydrate, amino acid, and energy, were upregulated in the iron-modified systems. The large proportion of potential genes involved in the metabolisms of amino acid and carbohydrate ensured significant removal of organic matter.<sup>51</sup> Furthermore, energetic systems such as phosphotransferase systems correlated with P removal and oxidative phosphorylation involved in adenosine triphosphate (ATP) formation<sup>52</sup> were enhanced in iron-modified reactors. Additionally, membrane transport, replication and repair, and cell motility functions belonging to environmental information, genetic information, and cellular processes, respectively, were powerful in the ACSI and ACFI systems. As an essential element of transport proteins,<sup>34</sup> iron is beneficial to the membrane transport function, which contains

various transporters (i.e., ATP-binding cassette transporters) and plays important roles in facilitating the translocation of various substrates (i.e., ions, sugars, proteins, etc.) across cytoplasmic membranes.<sup>53</sup> Thus, iron stimulated the interaction between pollutants and microbes.

Table 3 shows the forecasted functional gene abundance of specific key enzymes responsible for the nitrogen cycle based on KEGG database in the three systems. The effect of iron addition on key enzyme expression was not obvious in the sediment samples. As the main site of microbial denitrification, the gene coding for key enzymatic abundance in water samples was significantly improved by iron. The abundance of EC1.7.7.2 (formate-dependent nitrite reductase, periplasmic cytochrome *c552* subunit) and EC1.7.99.4 (nitrate reductase) related to transformation of nitrate to nitrite showed a significant increase by iron dosage. In the ACSI system, the abundance of EC1.7.7.1 (ferredoxin-nitrite reductase), EC1.7.1.15 (nitrite reductase), EC1.7.2.2 [nitrite reductase (cytochrome; ammonia-forming)], and EC1.7.99.1 (hydroxylamine reductase), which related to nitrite and hydroxylamine transformation to ammonia, was much higher than those in the other two systems. The variation in forecasted gene coding for key enzymes related to nitrogen reduction was consistent with the previous study of iron carbon base CW.<sup>23</sup> In addition, iron was reported to promote the activities of four biological nitrogen removal-related enzymes (AMO and NXR for nitrification, and NAP and NOR for denitrification) in activated sludge.<sup>28</sup> The potential mechanism of Fe/C micro-electrolysis carriers to enhance aerobic denitrification is that it can provide electrons to promote the electron transport activity of the microbial system, simultaneously improve four key denitrification enzymes (NAR, NIR, NOR, and NOS), and increase the accumulative abundance of denitrification genes.<sup>54</sup> The quantity of the key denitrifying functional gene *napA*-encoding enzyme NAP, which is necessary for aerobic denitrification, was obviously promoted by iron modification.<sup>28</sup> Overall, the higher relative abundance of specific microbial functions and forecasted key denitrifying functional genes in iron-modified systems indicated that iron was beneficial for aerobic denitrification, followed by an improvement in the specific pollutant removal capacity.

**3.6. Implications.** In this study, the iron-carbon carrier performed advantageously in terms of pollutant removal capacity in actual oligotrophic source water. According to a

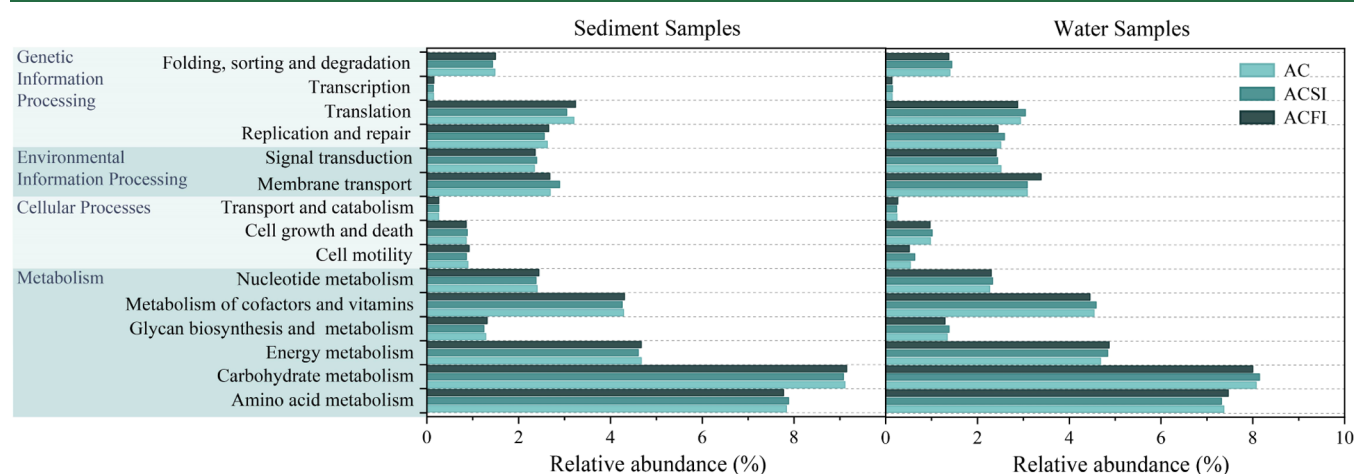


**Figure 6.** Predicted bacterial functions in AC, ACSI, and ACFI systems at the end of operation.

Table 3. Abundance of Nitrogen Cycle-Related Key Enzymes in AC, ACSI, and ACFI Systems at the End of Operation ( $10^{-2}$ )

enzyme	sediment samples			water samples		
	AC	ACSI	ACFI	AC	ACSI	ACFI
EC1.7.7.2	10.242	10.974	9.827	1.843	3.700	4.180
EC1.7.99.4	173.533	162.687	184.986	150.627	203.729	99.325
EC1.7.2.1	12.839	13.444	17.262	3.855	11.848	9.881
EC1.7.2.5	18.263	16.373	29.253	27.033	18.147	25.899
EC1.7.2.4	9.631	11.033	11.888	3.524	6.722	8.362
EC1.18.6.1	38.825	48.300	35.922	5.822	15.925	6.172
EC1.7.7.1	12.031	14.685	16.118	1.233	2.138	0.873
EC1.7.1.15	142.049	126.184	148.339	184.989	302.903	164.853
EC1.7.2.2	17.792	22.766	12.272	0.280	0.400	0.595
EC1.13.12.16	113.486	96.069	115.047	158.250	239.234	113.846
EC1.7.2.6	0.723	0.587	0.908	0.005	0.060	0.030
EC1.7.99.1	53.305	66.070	43.582	2.612	5.530	6.190
EC1.14.99.39	0.952	0.958	0.692	0.010	0.065	0.035
EC3.5.5.1	35.349	33.283	37.969	230.137	201.375	211.328

previous study,<sup>18</sup> Fe/AC micro-electrolysis can also perform certain in situ modifications to the properties of AC, leading to improved carrier performance. Moreover, this operation did not require complex equipment and costly material and resulted in negligible secondary pollution, which improved its feasibility for in situ remediation of source water.

However, many problems must be addressed. There is a probability of intergranular space blockage and surface cover occurring in iron or AC particulates by microorganisms in biotic systems,<sup>15</sup> iron-phosphorus precipitation on the exterior,<sup>23</sup> and (hydro)oxide coating formed under alkaline conditions.<sup>14</sup> These phenomena can lead to the blockage of the electron transfer required for nitrate reduction from ZVI oxidation and terminate the execution of eq 3, but also prevent the coprecipitation of phosphorus. This will subsequently weaken the pollutant removal ability of the system and render the added iron as waste. Similar to previous findings,<sup>9</sup> ZVI was not fully utilized at the end of the experiment as only a small amount of iron deposited into the sediments. A long-term study of reactor operation is also necessary to examine the stability of the system.

Future research should aim at prolonging the reaction and forming relatively stable dual biofilms (anaerobic inner layer and aerobic outer layer) on the surfaces of iron and AC, thereby allowing oxidized iron ions to be reduced to low-valent ions under anaerobic conditions that continue to provide electrons for aerobic denitrification. Furthermore, iron-reducing bacteria can convert ferric to ferrous iron and assist in the cycling of iron ions in different valence states; thus, future studies may combine them to enhance the removal of pollutants. In addition, this study proved that a combination of water-lifting aerators (artificial mixing and oxygenating equipment applied in reservoirs), and iron-carbon material enhances the aboriginal bacteria consortium and has a significant potential to treat micro-polluted waterbodies (i.e., urban lakes, rivers, and reservoirs) in situ.

## ■ ASSOCIATED CONTENT

### Supporting Information

The Supporting Information is available free of charge at <https://pubs.acs.org/doi/10.1021/acs.est.1c05254>.

Layout of an aerobic denitrifying reaction system; removal performance of AC, ACSI, and ACFI systems during the experimental operation; variations in  $\text{NO}_2^-$ -N

concentration and  $\text{NH}_4^+$ -N concentration; pH variations in AC, ACSI, and ACFI systems during the experimental operation; and water quality parameters of raw water, including the water temperature, the pH, and the concentrations of TN,  $\text{NO}_3^-$ -N,  $\text{NO}_2^-$ -N,  $\text{NH}_4^+$ -N, TP, and  $\text{COD}_{\text{Mn}}$  (PDF)

## ■ AUTHOR INFORMATION

### Corresponding Author

**Haihan Zhang** – Shaanxi Key Laboratory of Environmental Engineering, Key Laboratory of Northwest Water Resource, Environment and Ecology, MOE and School of Environmental and Municipal Engineering, Xi'an University of Architecture and Technology, Xi'an 710055, China; [orcid.org/0000-0001-8196-9881](https://orcid.org/0000-0001-8196-9881); Phone: +86-29-82202507; Email: [zhanghaihan@xauat.edu.cn](mailto:zhanghaihan@xauat.edu.cn); Fax: +86-29-82202729

### Authors

**Yuwei Huang** – Xi'an Weiyuan Environmental Protection and Technology Co., Ltd., Xi'an 710054, China; Faculty of Civil Engineering and Geosciences, Delft University of Technology, 2628 CN Delft, The Netherlands

**Xiang Liu** – Shaanxi Key Laboratory of Environmental Engineering, Key Laboratory of Northwest Water Resource, Environment and Ecology, MOE and School of Environmental and Municipal Engineering, Xi'an University of Architecture and Technology, Xi'an 710055, China

**Ben Ma** – Shaanxi Key Laboratory of Environmental Engineering, Key Laboratory of Northwest Water Resource, Environment and Ecology, MOE and School of Environmental and Municipal Engineering, Xi'an University of Architecture and Technology, Xi'an 710055, China

**Tinglin Huang** – Shaanxi Key Laboratory of Environmental Engineering, Key Laboratory of Northwest Water Resource, Environment and Ecology, MOE and School of Environmental and Municipal Engineering, Xi'an University of Architecture and Technology, Xi'an 710055, China

Complete contact information is available at: <https://pubs.acs.org/10.1021/acs.est.1c05254>

## Author Contributions

Y.H.: investigation, writing—original draft. H.Z.: conceptualization. X.L.: investigation. B.M.: investigation. T.H.: conceptualization.

## Notes

The authors declare no competing financial interest.

## ACKNOWLEDGMENTS

This study was supported by the National Nature Science Foundation of China (nos 51979217 and 52170012), the Grant from Youth Innovation Team of Shaanxi Universities in 2020 (PI: H.Z.), the key research and development innovation chain project of Shaanxi Province (no. 2019ZDLSF06-03), and the Youth Innovation Team of Shaanxi Universities (no. 21JP061).

## REFERENCES

- (1) Ma, Y.; Zheng, X.; Fang, Y.; Xu, K.; He, S.; Zhao, M. Autotrophic denitrification in constructed wetlands: Achievements and challenges. *Bioresour. Technol.* **2020**, *318*, 123778.
- (2) Huang, Y.; Yang, C.; Wen, C.; Wen, G. S-type dissolved oxygen distribution along water depth in a canyon-shaped and algae blooming water source reservoir: Reasons and control. *Int. J. Environ. Res. Publ. Health* **2019**, *16*, 987.
- (3) Zhang, H.; Ma, B.; Huang, T.; Shi, Y. Nitrate reduction by the aerobic denitrifying actinomycete *Streptomyces* sp. XD-11-6-2: Performance, metabolic activity, and micro-polluted water treatment. *Bioresour. Technol.* **2021**, *326*, 124779.
- (4) Ona-Nguema, G.; Guerbois, D.; Pallud, C.; Brest, J.; Abdelmoula, M.; Morin, G. Biogenic Fe(II-III) hydroxycarbonate green rust enhances nitrate removal and decreases ammonium selectivity during heterotrophic denitrification. *Minerals* **2020**, *10*, 818.
- (5) Wang, H.; Wang, T.; Yang, S.; Liu, X.; Kou, L.; Huang, T.; Wen, G. Nitrogen removal in oligotrophic reservoir water by a mixed aerobic denitrifying consortium: Influencing factors and immobilization effects. *Int. J. Environ. Res. Publ. Health* **2019**, *16*, 583.
- (6) Zhang, H.; Wang, Y.; Huang, T.; Liu, K.; Huang, X.; Ma, B.; Li, N.; Sekar, R. Mixed-culture aerobic anoxygenic photosynthetic bacterial consortia reduce nitrate: Core species dynamics, co-interactions and assessment in raw water of reservoirs. *Bioresour. Technol.* **2020**, *315*, 123817.
- (7) Robertson, L. A.; Kuenen, J. G. *Thiosphaera pantotropa* gen. nov. sp. nov., a facultatively anaerobic, facultatively autotrophic sulphur bacterium. *J. Gen. Microbiol.* **1983**, *129*, 2847–2855.
- (8) Tang, Y.; Li, M.; Xu, D.; Huang, J.; Sun, J. Application potential of aerobic denitrifiers coupled with a biostimulant for nitrogen removal from urban river sediment. *Environ. Sci. Pollut. Res.* **2018**, *25*, 5980–5993.
- (9) Su, Z.; Zhang, Y.; Jia, X.; Xiang, X.; Zhou, J. Research on enhancement of zero-valent iron on dissimilatory nitrate/nitrite reduction to ammonium of *Desulfovibrio* sp. CMX. *Sci. Total Environ.* **2020**, *746*, 141126.
- (10) Yang, L.; Ren, Y.-X.; Liang, X.; Zhao, S.-Q.; Wang, J.-p.; Xia, Z.-H. Nitrogen removal characteristics of a heterotrophic nitrifier *Acinetobacter junii* YB and its potential application for the treatment of high-strength nitrogenous wastewater. *Bioresour. Technol.* **2015**, *193*, 227–233.
- (11) Medhi, K.; Singhal, A.; Chauhan, D. K.; Thakur, I. S. Investigating the nitrification and denitrification kinetics under aerobic and anaerobic conditions by *Paracoccus denitrificans* ISTOD1. *Bioresour. Technol.* **2017**, *242*, 334–343.
- (12) Ma, B.; Zhang, H.; Ma, M.; Huang, T.; Guo, H.; Yang, W.; Huang, Y.; Liu, X.; Li, H. Nitrogen removal by two strains of aerobic denitrification actinomycetes: Denitrification capacity, carbon source metabolic ability, and raw water treatment. *Bioresour. Technol.* **2022**, *344*, 126176.
- (13) Zhou, S.; Zhang, Y.; Huang, T.; Liu, Y.; Fang, K.; Zhang, C. Microbial aerobic denitrification dominates nitrogen losses from reservoir ecosystem in the spring of Zhoucun reservoir. *Sci. Total Environ.* **2019**, *651*, 998–1010.
- (14) Lopes, D. V.; Sillanpää, M.; Wolkersdorfer, C. Nitrate reduction of the Siilinjärvi/Finland mine water with zero-valent iron and iron waste as alternative iron sources. *Mine Water Environ.* **2020**, *39*, 280–290.
- (15) Narayanasamydamodaran, S.; Zuo, J. e.; Ren, H.; Kumar, N. Scrap iron filings assisted nitrate and phosphate removal in low C/N waters using mixed microbial culture. *Front. Environ. Sci. Eng.* **2021**, *15*, 66.
- (16) Quan, X.; Zhang, H.; Liu, H.; Chen, L.; Li, N. Remediation of nitrogen polluted water using Fe-C microelectrolysis and biofiltration under mixotrophic conditions. *Chemosphere* **2020**, *257*, 127272.
- (17) Zhang, Y.; Douglas, G. B.; Kaksonen, A. H.; Cui, L.; Ye, Z. Microbial reduction of nitrate in the presence of zero-valent iron. *Sci. Total Environ.* **2019**, *646*, 1195–1203.
- (18) Feng, Q.; Guo, W.; Wang, T.; Cristina Macias Alvarez, L.; Luo, M.; Ge, R.; Zhou, C.; Zhang, Q.; Luo, J. Iron coupling with carbon fiber to stimulate biofilms formation in aerobic biological film systems for improved decentralized wastewater treatment: Performance, mechanisms and implications. *Bioresour. Technol.* **2021**, *319*, 124151.
- (19) Kim, I.; Cha, D. K. Effect of low temperature on abiotic and biotic nitrate reduction by zero-valent iron. *Sci. Total Environ.* **2021**, *754*, 142410.
- (20) Sun, Y.; Gao, K.; Zhang, Y.; Zou, H. Remediation of persistent organic pollutant-contaminated soil using biosurfactant-enhanced electrokinetics coupled with a zero-valent iron/activated carbon permeable reactive barrier. *Environ. Sci. Pollut. Res.* **2017**, *24*, 28142–28151.
- (21) Peng, S.; Kong, Q.; Deng, S.; Xie, B.; Yang, X.; Li, D.; Hu, Z.; Sun, S. Application potential of simultaneous nitrification/Fe<sup>0</sup>-supported autotrophic denitrification (SNAD) based on iron-scrap and micro-electrolysis. *Sci. Total Environ.* **2020**, *711*, 135087.
- (22) Li, S.; Zhang, H.; Huang, T.; Ma, B.; Miao, Y.; Shi, Y.; Xu, L.; Liu, K.; Huang, X. Aerobic denitrifying bacterial communities drive nitrate removal: Performance, metabolic activity, dynamics and interactions of core species. *Bioresour. Technol.* **2020**, *316*, 123922.
- (23) Huang, X.; Yang, X.; Zhu, J.; Yu, J. Microbial interspecific interaction and nitrogen metabolism pathway for the treatment of municipal wastewater by iron carbon based constructed wetland. *Bioresour. Technol.* **2020**, *315*, 123814.
- (24) Si, Z.; Song, X.; Wang, Y.; Cao, X.; Wang, Y.; Zhao, Y.; Ge, X.; Sand, W. Untangling the nitrate removal pathways for a constructed wetland- sponge iron coupled system and the impacts of sponge iron on a wetland ecosystem. *J. Hazard. Mater.* **2020**, *393*, 122407.
- (25) Song, N.; Xu, J.; Cao, Y.; Xia, F.; Zhai, J.; Ai, H.; Shi, D.; Gu, L.; He, Q. Chemical removal and selectivity reduction of nitrate from water by (nano) zero-valent iron/activated carbon micro-electrolysis. *Chemosphere* **2020**, *248*, 125986.
- (26) Zhao, Z.; Zhang, X.; Cheng, M.; Song, X.; Zhang, Y.; Zhong, X. Influences of iron compounds on microbial diversity and improvements in organic C, N, and P removal performances in constructed wetlands. *Microb. Ecol.* **2019**, *78*, 792–803.
- (27) Vavilin, V. A.; Rytov, S. V. Nitrate denitrification with nitrite or nitrous oxide as intermediate products: Stoichiometry, kinetics and dynamics of stable isotope signatures. *Chemosphere* **2015**, *134*, 417–426.
- (28) Chen, H.; Zhao, X.; Cheng, Y.; Jiang, M.; Li, X.; Xue, G. Iron robustly stimulates simultaneous nitrification and denitrification under aerobic conditions. *Environ. Sci. Technol.* **2018**, *52*, 1404–1412.
- (29) Yamashita, T.; Hayes, P. Analysis of XPS spectra of Fe<sup>2+</sup> and Fe<sup>3+</sup> ions in oxide materials. *Appl. Surf. Sci.* **2008**, *254*, 2441–2449.
- (30) Hu, X.; Chen, K.; Lai, X.; Ji, S.; Kaiser, K. Effects of Fe(III) on biofilm and its extracellular polymeric substances (EPS) in fixed bed biofilm reactors. *Water Sci. Technol.* **2016**, *73*, 2060–2066.
- (31) Rahman, M. M.; Roberts, K. L.; Warry, F.; Grace, M. R.; Cook, P. L. M. Factors controlling dissimilatory nitrate reduction processes

in constructed stormwater urban wetlands. *Biogeochemistry* **2019**, *142*, 375–393.

(32) Tang, X.; Wu, M.; Li, R. Phosphorus distribution and bioavailability dynamics in the mainstream water and surface sediment of the Three Gorges Reservoir between 2003 and 2010. *Water Res.* **2018**, *145*, 321–331.

(33) Lefevre, E.; Bossa, N.; Wiesner, M. R.; Gunsch, C. K. A review of the environmental implications of in situ remediation by nanoscale zero valent iron (nZVI): Behavior, transport and impacts on microbial communities. *Sci. Total Environ.* **2016**, *565*, 889–901.

(34) Wang, Y.; Lin, Z.; Wang, Y.; Huang, W.; Wang, J.; Zhou, J.; He, Q. Sulfur and iron cycles promoted nitrogen and phosphorus removal in electrochemically assisted vertical flow constructed wetland treating wastewater treatment plant effluent with high S/N ratio. *Water Res.* **2019**, *151*, 20–30.

(35) Hahn, M. W. Isolation of strains belonging to the cosmopolitan Polynucleobacter necessarius cluster from freshwater habitats located in three climatic zones. *Appl. Environ. Microbiol.* **2003**, *69*, 5248–5254.

(36) Boscaro, V.; Felletti, M.; Vannini, C.; Ackerman, M. S.; Chain, P. S. G.; Malfatti, S.; Vergez, L. M.; Shin, M.; Doak, T. G.; Lynch, M.; Petroni, G. Polynucleobacter necessarius, a model for genome reduction in both free-living and symbiotic bacteria. *Proc. Natl. Acad. Sci. U.S.A.* **2013**, *110*, 18590–18595.

(37) Liang, Z.; Sun, J.; Zhan, C.; Wu, S.; Zhang, L.; Jiang, F. Effects of sulfide on mixotrophic denitrification by Thauera-dominated denitrifying sludge. *Environ. Sci.: Water Res. Technol.* **2020**, *6*, 1186–1195.

(38) Ontiveros-Valencia, A.; Ilhan, Z. E.; Kang, D.-W.; Rittmann, B.; Krajmalnik-Brown, R. Phylogenetic analysis of nitrate-and sulfate-reducing bacteria in a hydrogen-fed biofilm. *FEMS Microbiol. Ecol.* **2013**, *85*, 158–167.

(39) Ma, R.-C.; Chu, Y.-X.; Wang, J.; Wang, C.; Leigh, M. B.; Chen, Y.; He, R. Stable-isotopic and metagenomic analyses reveal metabolic and microbial link of aerobic methane oxidation coupled to denitrification at different O<sub>2</sub> levels. *Sci. Total Environ.* **2021**, *764*, 142901.

(40) Yang, L.; Li, X.; Chu, Z.; Ren, Y.; Zhang, J. Distribution and genetic diversity of the microorganisms in the biofilter for the simultaneous removal of arsenic, iron and manganese from simulated groundwater. *Bioresour. Technol.* **2014**, *156*, 384–388.

(41) Demir, N. M. Experimental study of factors that affect iron and manganese removal in slow sand filters and identification of responsible microbial species. *Pol. J. Environ. Stud.* **2016**, *25*, 1453–1465.

(42) Qian, G.; Hu, X.; Li, L.; Ye, L.; Lv, W. Effect of iron ions and electric field on nitrification process in the periodic reversal bio-electrocoagulation system. *Bioresour. Technol.* **2017**, *244*, 382–390.

(43) Chang, J.; Mei, J.; Jia, W.; Chen, J.; Li, X.; Ji, B.; Wu, H. Treatment of heavily polluted river water by tidal-operated biofilters with organic/inorganic media: Evaluation of performance and bacterial community. *Bioresour. Technol.* **2019**, *279*, 34–42.

(44) Shu, D.; He, Y.; Yue, H.; Wang, Q. Metagenomic and quantitative insights into microbial communities and functional genes of nitrogen and iron cycling in twelve wastewater treatment systems. *Chem. Eng. J.* **2016**, *290*, 21–30.

(45) Lukhele, T.; Selvarajan, R.; Nyoni, H.; Mamba, B. B.; Msagati, T. A. M. Diversity and functional profile of bacterial communities at Lancaster acid mine drainage dam, South Africa as revealed by 16S rRNA gene high-throughput sequencing analysis. *Extremophiles* **2019**, *23*, 719–734.

(46) Lu, Y.; Zhang, W.; Li, Y.; Zhang, C.; Wang, L.; Niu, L.; Zhang, H. Microbial community shift via black carbon: Insight into biological nitrogen removal from microbial assemblage and functional patterns. *Environ. Res.* **2021**, *192*, 110266.

(47) Liu, Y.-J.; Gu, J.; Liu, Y. Energy self-sufficient biological municipal wastewater reclamation: Present status, challenges and solutions forward. *Bioresour. Technol.* **2018**, *269*, 513–519.

(48) Wu, L.; Yang, Y.; Chen, S.; Zhao, M.; Zhu, Z.; Yang, S.; Qu, Y.; Ma, Q.; He, Z.; Zhou, J.; He, Q. Long-term successional dynamics of microbial association networks in anaerobic digestion processes. *Water Res.* **2016**, *104*, 1–10.

(49) Douterelo, I.; Dutilh, B. E.; Arkipova, K.; Calero, C.; Husband, S. Microbial diversity, ecological networks and functional traits associated to materials used in drinking water distribution systems. *Water Res.* **2020**, *173*, 115586.

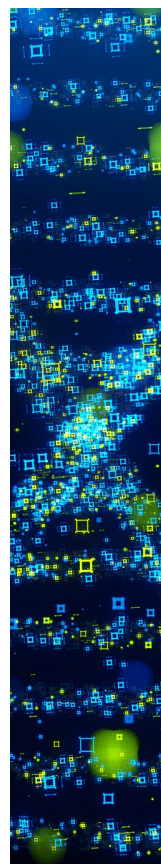
(50) Mougi, A.; Kondoh, M. Diversity of interaction types and ecological community stability. *Science* **2012**, *337*, 349–351.

(51) Liu, X.; Liu, Y.; Guo, X.; Lu, S.; Wang, Y.; Zhang, J.; Guo, W.; Xi, B. High degree of contaminant removal and evolution of microbial community in different electrolysis-integrated constructed wetland systems. *Chem. Eng. J.* **2020**, *388*, 124391.

(52) Xiang, Y.; Shao, Z.; Chai, H.; Ji, F.; He, Q. Functional microorganisms and enzymes related nitrogen cycle in the biofilm performing simultaneous nitrification and denitrification. *Bioresour. Technol.* **2020**, *314*, 123697.

(53) Maruyama, Y.; Itoh, T.; Kaneko, A.; Nishitani, Y.; Mikami, B.; Hashimoto, W.; Murata, K. Structure of a bacterial ABC transporter involved in the import of an acidic polysaccharide alginate. *Structure* **2015**, *23*, 1643–1654.

(54) Huang, L.; Chen, Y.; Ye, J.; Xiao, Y.; Tao, K.; Wang, Y.; Li, Y. Complete nitrogen removal from over-aeration treated black-odorous water via adding aerobic denitrifiers and iron-carbon micro-electrolysis carriers. *Chem. Eng. J.* **2022**, *433*, 133259.



CAS BIOFINDER DISCOVERY PLATFORM™

**STOP DIGGING  
THROUGH DATA  
—START MAKING  
DISCOVERIES**

CAS BioFinder helps you find the  
right biological insights in seconds

**Start your search**

